
**Separation Science and Technology**
Publication details, including instructions for authors and subscription information:
http://www.informaworld.com/smpp/title~content=t713708471

# Adsorptive Removal of Acid Blue 113 and Tartrazine by Fly Ash from Single and Binary Dye Solutions

Süheyla Pura[a]; Gülten Atun[a]
[a] Istanbul University, Department of Chemistry, Faculty of Engineering, Avcilar-Istanbul, Turkey

**To cite this Article** Pura, Süheyla and Atun, Gülten(2009) 'Adsorptive Removal of Acid Blue 113 and Tartrazine by Fly Ash from Single and Binary Dye Solutions', Separation Science and Technology, 44: 1, 75 — 101
**To link to this Article: DOI:** 10.1080/01496390802437057
**URL:** http://dx.doi.org/10.1080/01496390802437057

*Separation Science and Technology*, 44: 75–101, 2009

ISSN: 0149-6395 print/1520-5754 online
DOI: 10.1080/01496390802437057

Taylor & Francis
Taylor & Francis Group

# Adsorptive Removal of Acid Blue 113 and Tartrazine by Fly Ash from Single and Binary Dye Solutions

**Süheyla Pura and Gülten Atun**
Istanbul University, Department of Chemistry, Faculty of Engineering, Avcilar-Istanbul, Turkey



**Abstract:** Adsorption of two acid dyestuffs, acid blue 113 (AB) and tartrazine (TA), has been studied from their single and binary solutions by using fly ash (FA) as an adsorbent. The S shaped isotherms observed for dye adsorption from single solutions show that both acid dyes are not preferred at a low concentration region whereas adsorption of the dyes from binary solutions is enhanced via solute-solute interactions. Although the L-shaped isotherm is observed in binary solutions adsorbability of AB decreases in concentrated solutions with respect to single one, time dependency of adsorption is well described with a pseudo-second-order kinetic model as well as the linear relation of $Bt$ vs. $t$ plots (not passing through origin) indicates that film diffusion is effective on dye adsorption. Modeled isotherm curves using isotherm parameters of the Freundlich and Dubinin-Radushkevich (D-R) equations adequately fit to experimental equilibrium data. Equilibrium adsorption of AB in binary solutions has been quite well predicted by the extended Freundlich and the Sheindorf-Rebuhn-Sheintuch (SRS) models. In general, the isotherm curves constructed in the temperature range of 298–328 K show that the optimum temperature is 318 K for AB removal from both single and binary solutions.

**Keywords:** Acid blue 113, acid dyes, adsorption, fly ash, tartrazine

Received 10 January 2008; accepted 9 June 2008.
Address correspondence to Gülten Atun, Istanbul University, Department of Chemistry, Faculty of Engineering, 34320 Avcilar-Istanbul, Turkey. E-mail: gultena@istanbul.edu.tr

## INTRODUCTION

Many dyes present in industrial effluents are not readily degraded because of their complex aromatic structures. They create odor, bad taste, and unsightly color and cause carcinogenic effects on human and animal health. Acid dyes having a large anionic colored component are more problematic than basic and disperse dyes because anions are very weakly retained by most of the soil components due to their structural negative charge (1). Thus, they remain dissolved in the soil solution and can rapidly move around leading subsequent contamination of surface and ground waters. Adsorption is an effective and economic treatment technique to reduce dye concentration to desired- and/or legislated levels. There has been a growing interest in the developing of low cost special adsorbents from industrial byproducts including some ashes such as coal fly ash (2–14), bottom ash (15), rice husk ash (16), and bagasse fly ash (17–19).



Fly ash (FA) is a major solid waste material generated in coal-based thermal power plants produced annually 12.5 million tons in Turkey (20). Fly ashes of different origin have different sorption potentials for basic (2–12), acid (2–4,13), and reactive dyes (13,14). In general, the adsorption ability of fly ashes has been compared using methylene blue (MB) as a reference dye (2–9). The removal capacities of FA adsorbents for other basic dyes such as rhodamineB (2,5,12), crystal violet (5,9), toluidne blue (10), and chrysoidine R (11); acid dyes, egacid orange II, egacid red G, egacid yellow G, midlon black VL (2), congo red (3), alizarin sulfonate (AS) (4). Lanasyam Brown Grl (13) and reactive dyes, Verofix Red (13) and Reactive Black 5 have been reported in the literature. Adsorption capacity for acid-, basic- and reactive dyes depend on both the origin of FA and the molecular structure of the dye. For example, a FA sample shows slightly higher affinity for different acid dyes compared to basic dyes (2), while another sample has higher affinity for MB rather than AS (4).

Acid blue 113 (AB) existing in textile effluents coming from the nylon dying process has been removed using both $UV/H_2O_2$ decolorization (21) and adsorption processes (22). Although tartrazine (TA) is used as a cosmetic, drug, and food coloring dye it is considered highly toxic for humans due to high amounts in industrial effluents because of its high solubility. The removal capacity of some adsorbents for TA such as different types of carbon (23), bottom ash, de-oiled soya (24), magnesium–palladium system (25), hen feathers (26), and ion exchange resins (27,28) has been reported. It has been shown that TA selectively displaces with some proteins on an anion exchanger, source 15Q (28).

Although fly ash has been extensively used for dye adsorption, at least to our knowledge, dye removal by fly ash from binary solutions has not been studied before. The aim of this paper is to examine and compare single and binary adsorption of Acid blue 113 and tartrazine dyes onto fly ash.

## EXPERIMENTAL

### Adsorbate Specifications

Molecular structures of Acid Blue 113 and Tartrazine (FD&C Yellow No. 5) are presented in Fig. 1. AB obtained from Aldrich has a solubility of 40 g/l (21). TA was supplied from Sigma (St. Louis, MO, USA). Its solubility is 200 g/l at 298 K (24,26,27).



### Adsorbent Preparation and Specifications

The fly ash sample used as an adsorbent in this study was obtained from Ankara Çayirhan Thermal Power Plant in Turkey that is fuelled with Beypazari lignite. The chemical composition of the raw FA has been determined using RIGAKU RIX2000 X-Ray Fluorescence (XRF) spectrometer. The following oxides are involved in w/w%: $SiO_2$, 41.30;

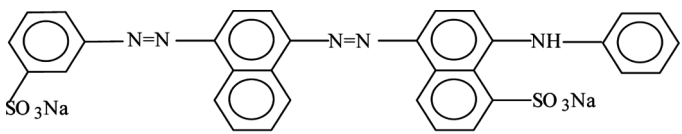


Acid Blue 113

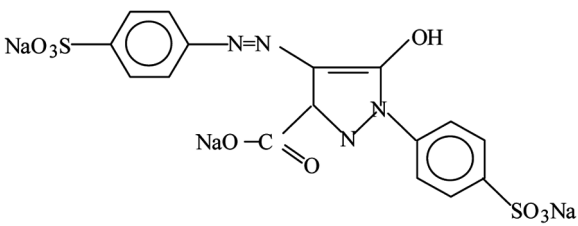


Tartrazine

***Figure 1.*** Chemical structure of two acid dyestuffs.

CaO, 16.3; $Al_2O_3$, 12.30; $Fe_2O_3$, 11.30; $K_2O$, 5.62; MgO, 4.10; $SO_3$, 5.43; $Na_2O$, 1.43; $TiO_2$, 0.981; $P_2O_5$, 0.625; MnO, 0.135; NiO, 0.092; SrO, 0.090; $Cr_2O_3$, 0.069; $ZrO_2$, 0.058; $V_2O_5$, 0.055; $As_2O_3$, 0.037; ZnO, 0.026; CuO, 0.013; $Rb_2O$, 0.012; PbO, 0.008; $Nb_2O_5$, 0.005; LOI, 0.00.

Mainly quartz and mullite minerals have been identified as crystalline phases in the glass forming fly ash (10). In scanning electron micrograph (SEM) studies, it has been shown that the average particle size of spherically shaped powder particles is about 3 μm (20).

20 g of FA was added to 2-liter distilled water and stirred for two hours until constant solution conductivity was attained. FA was separated by filtration and dried at 378 K for 24 hour before using as adsorbent. The chemical composition of the FA after water treatment is as follows (10): $SiO_2$, 43.40; CaO, 14.70; $Al_2O_3$, 12.80; $Fe_2O_3$, 11.60; $K_2O$, 5.68; MgO, 4.91; $SO_3$, 3.40; $Na_2O$, 1.24; $TiO_2$, 1.05; $P_2O_5$, 0.679; MnO, 0.187; NiO, 0.095; SrO, 0.088; $Cr_2O_3$, 0.075; $ZrO_2$, 0.062; $V_2O_5$, 0.052; $As_2O_3$, 0.030; ZnO, 0.026; CuO, 0.012; $Rb_2O$, 0.011; PbO, 0.010; $Nb_2O_5$, 0.004; LOI, 0.00. BET surface area and the point of zero charge of the FA are 7.1 $m^2/g$ and 2.1, respectively (10). Filtrate was used for preparation of dye solutions in order to avoid any changes of UV spectra during sorption experiments because of interactions of soluble components of FA with dye molecules. The concentrations of soluble heavy metals in the leachate do not exceed regulatory limits (10).



## Kinetic Studies

Time dependent studies were performed for the determination of equilibration time in dye adsorption process. The upper concentration limit is 0.4 mM for studying AB adsorption because of solubility problems in the solutions equilibrated with FA. Adsorption kinetics of AB was studied at 0.1, 0.2, and 0.4 mM initial concentrations. Although TA has a high solubility it is hardly adsorbed on FA in the solutions above 0.2 mM. Thus, time dependency of TA adsorption was studied in 0.1 and 0.2 mM dye solutions. In order to study binary sorption kinetics, equal volumes of dye solutions were mixed to give the final TA concentrations of 0.1 mM and 0.2 mM.

50 milliliters of dye solution at a given concentration were placed in a water jacketed Pyrex cell at 298 K. Solutions were continuously stirred with a magnetic stirrer after adding 0.5 g of FA. The solutions sampled in various time intervals were separated by centrifugation at 7000 rpm. Concentrations of the solutions were measured using Perkin Elmer 554 UV spectrophotometer. UV spectra were recorded in the wavelength

range of 200–700 nm employing quartz quvettes with a pathway of 1 cm. The concentrations of AB and TA in their individual solutions were determined from the peaks located at around a $\lambda_{max}$ of 520 and 420 nm, respectively. The peak of AB shifted to 544 nm in binary solutions. Absorbances of the AB and TA peaks located at 544 nm and 420 nm show a linear dependence on concentration in binary solutions. Concentrations of AB and TA in binary solutions were determined from their respective absorbances.

Amount of dye adsorbed at any time was calculated from the concentration changes during adsorption process as follows:

$$q_t = (C_0 - C_t)\frac{V}{m} \quad (1)$$

Where, $q_t$ is amount of the dye adsorbed (in mmol/g, i.e., mol/kg), $C_0$ and $C_t$ are dye concentrations at initial and time $t$ (in mM, i.e., mol/m$^3$) and $V/m$ is the ratio of the solution to the mass of adsorbent (in l/g, i.e., m$^3$/kg).

A slower process follows the initial fast process. Although adsorption is very fast up to 5 min. the adsorption equilibrium is established in a week. Adsorption data up to 30 minutes were used for kinetic calculations whereas relevant data for constructing the adsorption isotherms could be obtained from the concentration measurements at the end of a week.



## Equilibrium Studies

AB solutions in the concentration range of 0.05–0.40 mM were shaken with FA at a constant solution/solid ratio of 0.1 l/g in a thermostatic shaker for 4 hours, then intermittently agitated during a week until the establishment of equilibrium. The initial and final pH values of AB solutions were around 9.6 and 9.2, respectively. The suitable concentration range for studying single TA adsorption was 0.05–0.20 mM. The values of pH increased from 9.4 to 10.2 during adsorption experiments in TA solutions. Dye adsorption from binary solutions was studied in the concentration range of 0.05–0.30 mM AB in the presence of 0.05 and 0.10 mM TA under similar conditions. The values of initial and final pH of the mixed solutions were in the range of 7.9–8.1.

In order to evaluate thermodynamic parameters, all equilibrium experiments were performed at the temperatures of 298, 308, 318, and 238 K.

## RESULTS AND DISCUSSION

### Adsorption Kinetics

Time dependency of adsorption data obtained from single and binary solute adsorption has been tested in terms of some well-known kinetic equations and the best fit is obtained for the pseudo-second-order kinetic model proposed by Ho and McKay (29,30). The linearity test of *Bt* vs. *t* plots proposed by Boyd et al. and Reichenberg has also been employed to calculate effective diffusion coefficients corresponding to external transport or intraparticle-transport controlled rates of dye sorption process (31,32).

### Pseudo-Second-Order Kinetic Model



Representative $q_t$ vs. $t$ curves for 0.2 mM AB and 0.1 mM TA obtained from single and binary solutions are shown in Fig. 2a. The data well fit to the pseudo-second-order kinetic model represented as follows:

$$\frac{dq_t}{dt} = k_2(q_e - q_t)^2 \tag{2}$$

where, $k_2$ is the pseudo-second-order rate constant (in g/mmol s) and $q_e$ is the amount of dye adsorbed at equilibrium conditions (in mmol/g).

The integration of Eq. (2) results in following equation:

$$q_t = \frac{k_2 q_e^2 t}{1 + k_2 q_e t} \tag{3}$$

The boundary conditions are $q_t = 0$ at t = 0 and $q_t = q_t$ at $t = t$.

Since a plot constructed between $t/q_t$ and t according to the following linear relation yields always perfect correlation kinetic data must be calculated from the non-linear regression method (33).

$$\frac{t}{q_t} = \frac{1}{k_2 q_e^2} + \frac{1}{q_e} t \tag{4}$$

The initial sorption rate $h_s = k_2 q_e^2$ and $k_2$ have been correlated to the initial dye concentration as follows:

$$k_2 = \frac{C_0}{aC_0 + b} \tag{5}$$

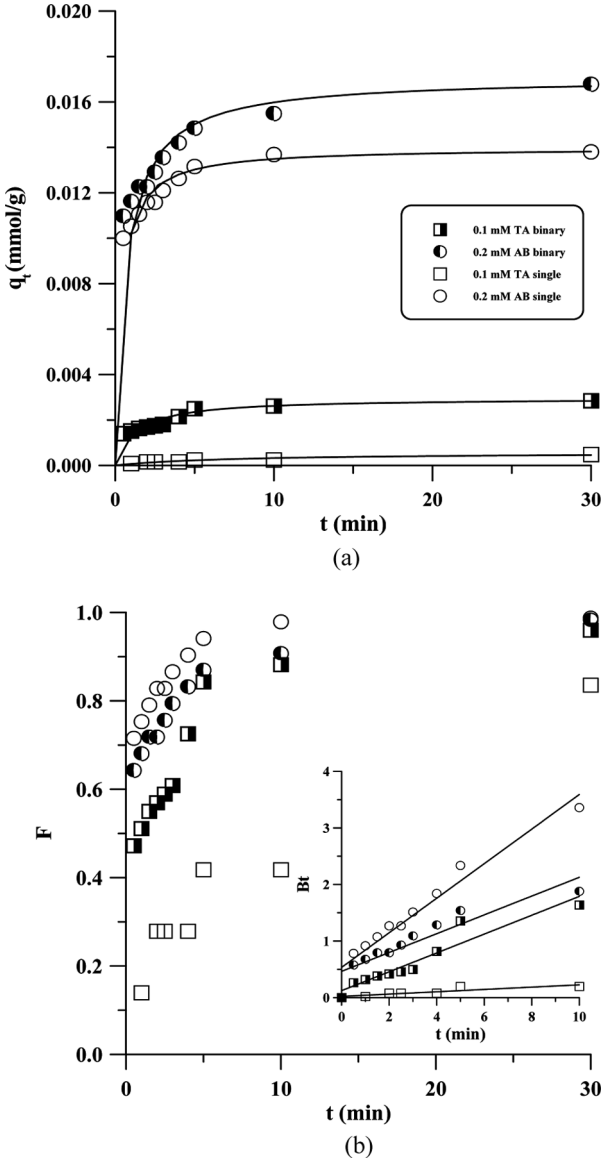


***Figure 2.*** Plots for evaluation of kinetic parameters: (a) Time dependencies of dye adsorbed from single AB, single TA and their binary solutions at selected concentrations. (b) Time dependencies of fractional attainment at equilibrium and evaluation of *Bt* vs. *t* plots for calculation of diffusion coefficients (in the inset).

$$h_s = \frac{C_0^2}{\alpha C_0 + \beta b} \tag{6}$$

The pseudo-second-order kinetic parameters, $q_e$, $k_2$, and $h_s$ together with $a$, $b$, $\alpha$, and $\beta$, have been calculated by minimizing standard deviations between experimental and calculated values of $q_t$ according to the following relation:

$$\sigma = \left[ \frac{1}{n_e - 2} \sum_{i=1}^{n} \left( \frac{q_{t,\exp} - q_{t,cal}}{q_{t,\exp}} \right)^2 \right]^{1/2} \tag{7}$$

where, $n_e$ is the number of experimental observations, subscripts "exp" and "cal" represent the experimental and calculated values of the dye adsorbed.

As it is seen from the kinetic parameters presented in Table 1, amount of AB adsorbed at equilibrium conditions increase from 7.50 mmol/g to 24.21 mmol/g as initial concentrations increase the 0.1–0.4 mM range. Their $k_2$ values also increase from $1.83 \times 10^2$ to $2.11 \times 10^2$ g/mmol s in the same concentration range showing the best fit to the model. Similar trends are also observed for single TA adsorption but the values of $q_e$ are lower than those of AB. This may be arising from the difference of the chemical structures and orientations of two dyes. Although both of the dyes involve in two sulphonate groups TA charges more negatively than AB when it ionizes in aqueous solutions because of its additional carboxylate and phonolate groups. More efficient coulombic repulsion forces between the TA molecules and the adsorbent surface may be responsible for the lower uptake TA. However, the $q_e$ values for both AB and TA in binary solutions are higher than those obtained from their single solute adsorption suggesting that solute-solute interactions between AB and TA enhance their adsorption ability under these conditions.



## Diffusion Coefficients

Assuming that all adsorbent particles are uniform spheres of radius $r$, the expression developed by Boyd et al. for the diffusion-controlled kinetics is as follows:

$$F_t = \frac{q_t}{q_e} = 1 - \frac{6}{\pi^2} \sum_{n=1}^{\infty} \frac{e^{-n^2 Bt}}{n^2} \tag{8}$$

Where, $F_t$ is the fractional attainment at equilibrium.

**Table 1.** Pseudo-second-order kinetic parameters and effective diffusion coefficients

| | $C_0$ mM | $q_{e\ \exp} \times 10^3$ mmol/g | $q_{e.cal} \times 10^3$ mmol/g | $k_2 \times 10^{-2}$ g/mmol s | $h_s \times 10^2$ mmol/g s | $a \times 10^3$ | $b \times 10^4$ | $\alpha$ | $\beta$ | $\sigma$ | $D_i \times 10^{15}$ $m^2/s$ | $r$ |
|---|---|---|---|---|---|---|---|---|---|---|---|---|
| AB single | 0.1 | 7.30 | 7.50 | 1.83 | 1.020 | 4.500 | 1.0 | 0.1 | 0.97 | 0.010 | 0.54 | 0.92 |
| | 0.2 | 13.80 | 14.10 | 1.92 | 3.850 | 4.700 | 1.0 | 0.2 | 1.00 | 0.001 | 1.16 | 0.97 |
| | 0.4 | 24.21 | 25.00 | 2.11 | 13.110 | 3.500 | 5.0 | 0.3 | 1.10 | 0.001 | 1.48 | 0.98 |
| TA single | 0.1 | 0.48 | 0.57 | 2.20 | 0.007 | 0.139 | 1.8 | 0.05 | 1.44 | 0.057 | 0.08 | 0.88 |
| | 0.2 | 3.67 | 3.67 | 5.15 | 0.694 | 0.190 | 3.5 | 0.32 | 5.70 | 0.001 | 0.99 | 0.73 |
| AB binary | 0.2 | 16.77 | 17.07 | 0.86 | 2.499 | 10.000 | 3.33 | 0.0035 | 1.60 | 0.008 | 0.63 | 0.92 |
| TA binary | 0.1 | 2.84 | 2.96 | 2.63 | 0.226 | 0.510 | 3.30 | 0.5500 | 4.30 | 0.004 | 0.63 | 0.95 |

Integrating of Eq. (8) with respect to $Bt$ gives following equation:

$$F_t = \frac{6}{\pi^{3/2}}(Bt)^{1/2} - \frac{3}{\pi^2}(Bt) + \frac{6}{\pi^{3/2}}\int_0^{Bt} \frac{\sum_{n=1}^{\infty} \frac{e^{-n^2 Bt}}{n^2}}{(Bt)^{1/2}} \tag{9}$$

The third term is neglected and only the first two terms are considered for calculation of $Bt$ for low $F_t$ values up to 0.85. At higher $F_t$ values the relation is given as follows:

$$F_t = 1 - \frac{6}{\pi^2} e^{-Bt} \tag{10}$$

where, $B$, the time coordinate, is defined by:

$$B = \frac{\pi^2}{r^2} D_i \tag{11}$$

here, $D_i$ is the effective diffusion coefficient of the adsorbing ions.

The $F_t$ values derived from the data in Fig. 2a are plotted vs. $t$ in Fig. 2b. For every observed value of $F_t$, corresponding $Bt$ values, as derived from above Eqs. (9) and (10), can also be obtained from the Reichenberg table (32). It can be seen from the inset in Fig. 2b, $Bt$ vs. $t$ plots are linear but do not pass through the origin except for 0.1 mM TA, indicating that, film-diffusion mainly governs the rate-limiting process. The straight-line passing through the origin implies that the adsorption rate of TA in single solution is controlled by particle diffusion whilst film-diffusion is the rate limiting step in binary solutions. It has been reported that TA adsorption on bottom ash, deoiled soya, and hen feather is dominated by film-diffusion at low concentrations whereas the particle diffusion takes place at high concentrations of dye solutions (15,24).

The effective diffusion coefficients calculated according to Eq. (10) using the average particle radius of 1.5 μm are also presented in the Table 1 for studied systems. The values of $D_i$ in Table 1 fall in the range of $8.0 \times 10^{-17}$–$1.48.0 \times 10^{-15}\,m^2/s$, which are within the ranges for chemisorption systems ($10^{-21}$–$10^{-13}\,m^2/s$) (33). They are less than the reported values of effective diffusion coefficients for TA adsorption on bottom ash and deoiled soya of $1.809 \times 10^{-9}\,m^2/s$ and $3.179 \times 10^{-13}\,m^2/s$, respectively. This implies that the magnitude of diffusion coefficients strongly depends on the nature of the adsorbent. The diffusion coefficients in the present systems may also be reduced by the formation of large-size dye aggregates.

## Adsorption Equilibria

### AB Adsorption in Single Solute System

The adsorption isotherms of AB obtained from the equilibrium data in the different temperature range of 298–328 K are depicted in Fig. 3a. As is seen from Fig. 3a, an S shaped isotherm is observed at low concentrations. The curves shift towards the left side as the temperature increases up to 308 K while a reverse temperature effect is observed at 328 K.

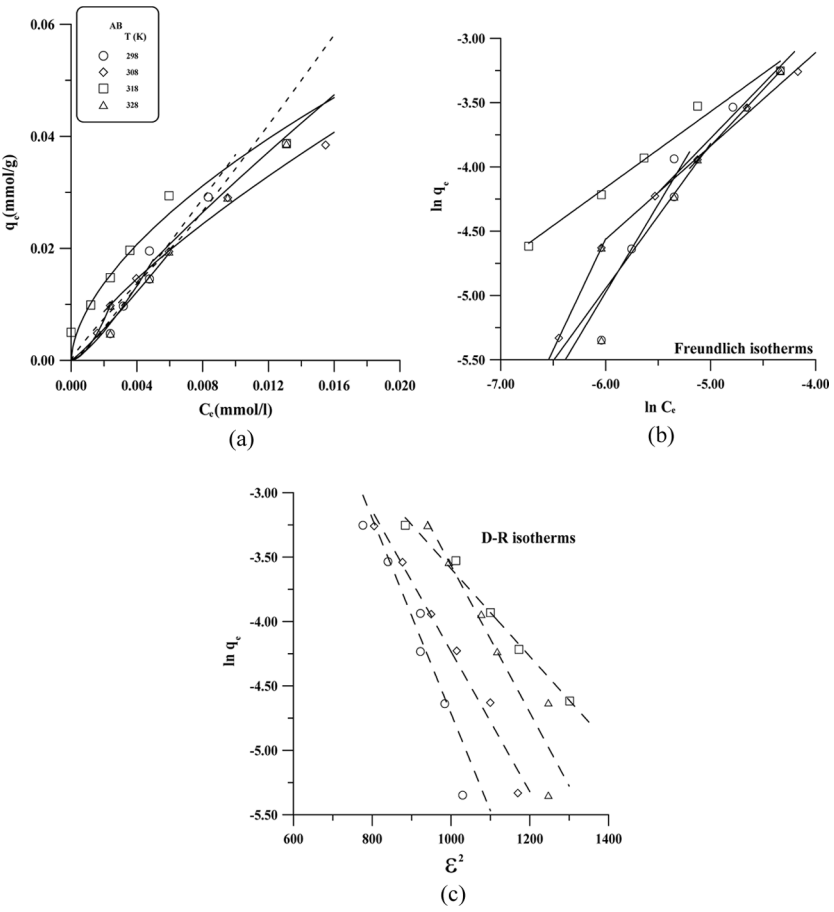


***Figure 3.*** (a) Adsorption isotherms -, (b) Freundlich and (c) (D-R) isotherm plots - of AB at different temperatures. (Solid and dashed curves in (a) were calculated from Freundlich and D-R models, respectively.).

The data presented in Fig. 3a were analyzed according to the Freundlich and the Dubinin-Radushkevich (D-R) isotherm equations. The Freundlich adsorption isotherm can be written as follows:

$$q_e = k_F C_e^n \tag{12}$$

where, $k_F$ is the Freundlich constant, which is a comparative measure of the adsorption capacity of the adsorbent, and $n$ is an empirical constant which gives valuable information about the isotherm shape. The $n > 1$ value represents an S shaped isotherm with a concave profile at initial which is an indication of unfavorable adsorption. The value of $n = 1$ corresponds to a C-shaped isotherm curve which is strictly linear whereas the value of $n < 1$ indicates favorable adsorption having a convex isotherm profile. The convex isotherms are classified as the L- and H-shaped. When $n$ value closes to 0 an L shaped isotherm converts into H shaped.

The Freundlich parameters can be obtained from the following linearized equation:

$$\ln q_e = \ln k_F + n \ln C_e \tag{13}$$

As shown in Fig. 3b, a plot of $\ln q_e$ vs $\ln C_e$ gives two straight lines having lower slope in the second part. As is seen from Table 2, the Freundlich exponents $n$ corresponding to the initial part of the isotherm are higher than unity whereas $n' < 1$. These results imply that AB adsorption onto FA is more favorable at higher concentrations. It can be concluded that the adsorption of acid dye AB is initiated by hydrophobic interactions between the solute and the adsorbent rather than the electrostatic one because of negative surface charge of the adsorbent under



**Table 2.** Freundlich and D-R isotherm parameters for AB adsorption from single solute system

| | | Freundlich parameters | | | | | D-R parameters | | |
|---|---|---|---|---|---|---|---|---|---|
| $T$ (K) | $n$ | $k_F$ mmol/g | $r$ | $n'$ | $k'_F$ mmol/g | $r$ | $K_{D\text{-}R} \times 10^3$ mol$^2$/kJ$^2$ | $q_m$ mmol/g | $r$ |
| 298 | 1.36 | 24.88 | 0.91 | 0.84 | 1.55 | 0.95 | 7.56 | 17.32 | 0.96 |
| 308 | 1.73 | 340.02 | 1.00 | 0.73 | 0.81 | 1.00 | 5.44 | 3.36 | 0.99 |
| 318 | – | – | – | 0.59 | 0.54 | 0.99 | 3.40 | 0.83 | 0.99 |
| 328 | 1.13 | 6.13 | 0.88 | 0.87 | 1.71 | 1.00 | 5.71 | 8.50 | 0.95 |

experimental conditions. Then, solute-solute interactions at higher concentrations play more important role on adsorption mechanisms.

The D-R isotherm equation can be useful for the calculation of adsorption capacity ($q_m$) when solute-solute interactions on the adsorbent are important. The D-R isotherm equation and its linear form can be written as follows:

$$q_e = q_m e^{-K_{D-R}\varepsilon^2} \tag{14}$$

$$\ln q_e = \ln q_m - K_{D-R}\varepsilon^2 \tag{15}$$

where, $K_{D\text{-}R}$ is the constant related to the mean adsorption energy and $\epsilon$ is the Polanyi potential:

$$\varepsilon = RT\ln(1 + 1/C_e), \tag{16}$$

where, $R$ is the gas constant and $T$ is the absolute temperature.

The mean adsorption energy is defined as the free energy change when one mole of solute is transferred to the adsorbent surface from infinity in the solution and it can be estimated using constant K as follows:

$$E = (2K_{D-R})^{-1/2} \tag{17}$$

As it is seen in Fig. 3c, a plot of $\ln q_e$ vs. $\varepsilon^2$, allows the estimation of $q_{\mathrm{m}}$ from the intercept and $K_{D\text{-}R}$ from the slope, respectively. The D-R constants in Table 2 show that the predicted adsorption capacity for the L-shaped isotherm at 308 K is 0.83 mmol/g. The higher capacities at other temperatures arise from solute-solute interactions at higher concentrations. Unfortunately, it could not be attained to the predicted adsorption capacities under experimental conditions because AB precipitates in higher solute concentrations than 0.4 mM. However, its experimentally observed value of $3.9 \times 10^{-2}$ mmol/g is higher than the reported adsorption capacities for other acid dyes on a FA from a plant used brown coal such as egacid orange II, egacid red G, egacid yellow G and midlon black VL of $4.7 \times 10^{-3}$, $2.2 \times 10^{-3}$, $1.5 \times 10^{-3}$ and $1.5 \times 10^{-3}$ mmol/g, respectively (2). The adsorption capacity of a fly ash obtained a plant fuelled with lignit coal has been reported as $6.3 \times 10^{-3}$ mmol/g for CR (3) whereas a modified FA with NaOH has a capacity for AS of $7.13 \times 10^{-3}$ mmol/g (4).

Theoretical isotherm curves calculated using the Freundlich and the D-R constants in Table 2 are compared to experimental data points in Fig. 3a. Both of the isotherm equations are able to adequately predict the equilibrium behavior of single AB adsorption.

## TA Adsorption in Single Solute System

Adsorption isotherms of TA on FA are shown in Fig. 4. The experimental data were fitted to Freundlich and D-R equations and the isotherm constants presented in Table 3 are used for the calculations of theoretical isotherm curves. Although both Freundlich and D-R curves are in accordance with experimental data $k$ and $q_m$ values presented in Table 3 can not be correlated to the adsorption capacity of the adsorbent. An S shaped isotherm is typical for surfactant adsorption. Four-region or reverse orientation model has been proposed for interpretation of the straight lines in $\ln q_e - \ln C_e$ plot of a completed S shaped isotherm (34–36). In region I corresponding to the lowest concentrations, the surfactant monomers are adsorbed with head groups and their tail groups interact with any hydrophobic regions of the adsorbent surface. Region II involves strong lateral interaction between adsorbed monomers, resulting in the formation of primary aggregates at higher concentrations. Increases in the amount of surfactant adsorbed in region III are thought

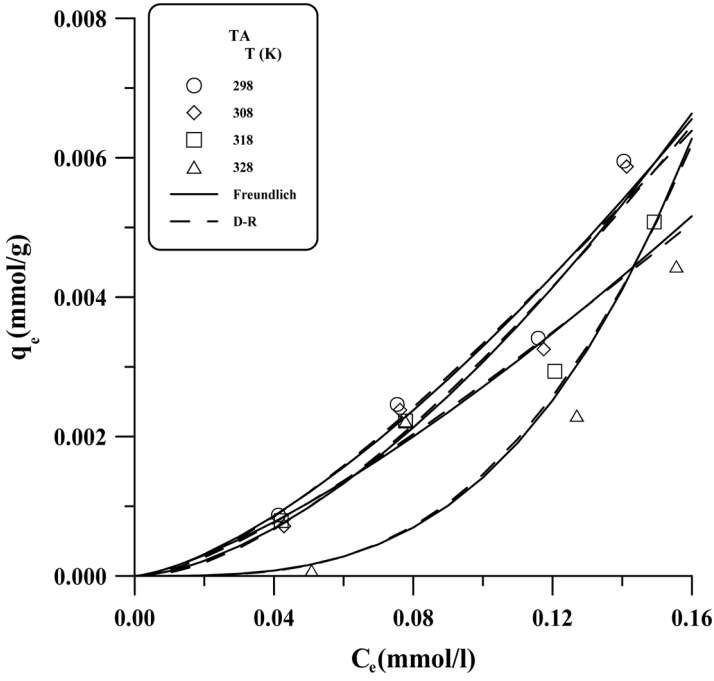


***Figure 4.*** Adsorption isotherms of TA at different temperatures. (Solid and dashed curves were calculated from Freundlich and D-R models, respectively.).

**Table 3.** Freundlich and D-R isotherm parameters for TA adsorption from single solute system

| | Freundlich Parameters | | | D-R Parameters | | |
|---|---|---|---|---|---|---|
| $T$ (K) | $n$ | $k_F$ mmol/g | $r$ | $K_{D\text{-}R} \times 10^3$ mol$^2$/kJ$^2$ | $q_m$ mmol/g | $r$ |
| 298 | 1.46 | 0.10 | 0.99 | 1.25 | 2.31 | 0.99 |
| 308 | 1.64 | 0.13 | 0.98 | 1.32 | 4.88 | 0.98 |
| 318 | 1.37 | 0.06 | 0.98 | 1.03 | 1.28 | 0.98 |
| 328 | 3.18 | 2.11 | 0.88 | 2.30 | 3016.94 | 0.89 |



to result from the growth of the structures formed in region II, without any increase in the number of surface aggregates. Adsorption capacity can be calculated from the intercept of the staight line of region IV that the surface morphology is assumed to be a fully formed bilayer (37). Adsorption of organic dyes can also be explained based on this model (10). Since TA was not adsorbed above 0.2 mM initial concentrations only the initial part of an S shaped isotherm could be observed. This result suggests that TA molecules exist in monomer form at the low concentrations while at higher concentrations dimers or higher dye aggregates might occur. Monomer dye molecules adsorbed on FA behave as nucleation sites for TA adsorption via solute-solute interactions in dilute solutions whereas these interactions might be higher in solution phase in more concentrated solutions than 0.2 mM TA. Similar behavior has been observed for adsorption of some organic molecules having phenolic moiety (38). It can be concluded from Fig. 4, adsorption ability of FA of $5.9 \times 10^{-3}$ mmol/g for TA is comparable to the adsorption capacities reported for other acid dyes (2–4).

## AB and TA Adsorption in Binary Solutions

Adsorption isotherms of AB in the presence of 0.05 and 0.10 mM TA are depicted in Figs. 5a and 5b, respectively. It can be concluded from the figures and from the Freundlich exponents ($n < 1$) presented in Table 4 AB adsorption from binary solutions are favorable at the whole temperature range. A comparison of $n$ values in Tables 2 and 4 indicates that AB adsorption in binary system at low concentration region is more preferential than the single one. However, the maximum values of the adsorbed amount under experimental conditions are

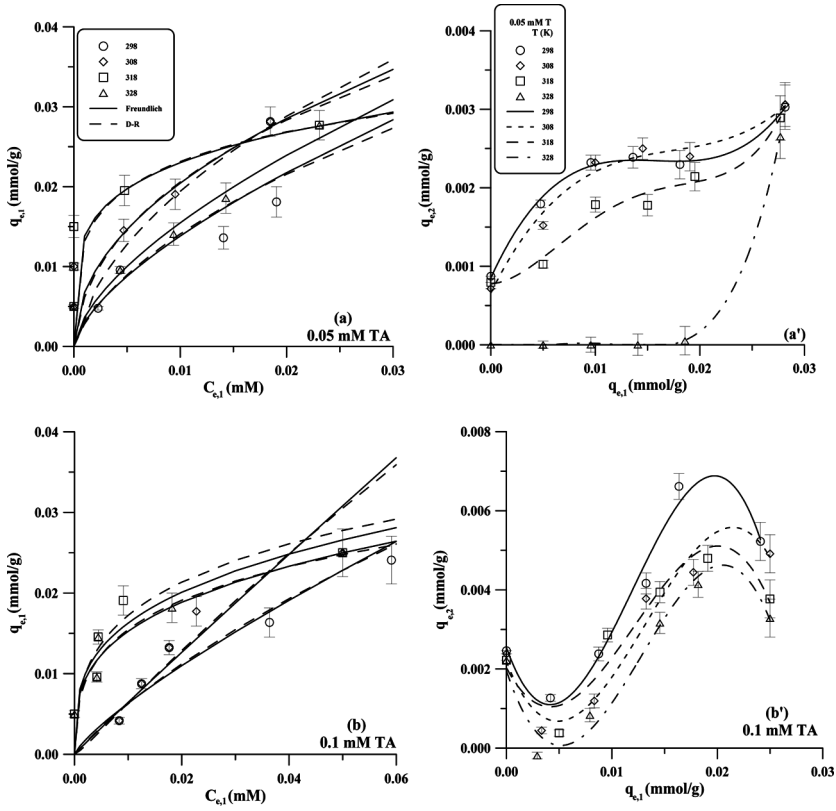


***Figure 5.*** Adsorption isotherms of AB (a) in the presence of 0.05 mM TA- and (b) in the presence of 0.10 mM TA, (a′) Polynomial relation between TA and AB adsorbed in the presence of 0.05 mM TA- and (b′) in the presence of 0.10 mM TA at different temperatures. (Solid and dashed curves in (a) and (b) were calculated from Freundlich and D-R models, respectively.).

$2.8 \times 10^{-2}$ and $2.5 \times 10^{-2}$ mmol/g in the presence of 0.05 and 0.10 mM TA indicating that the AB adsorption from the single solution is more favorable than binary solutions at higher concentrations than 0.2 mM AB. These results suggest that solute-solute interaction between AB and TA molecules on the adsorbent surface are less favorable in concentrated solutions.

Equilibrium isotherms of AB in the presence of TA have also been analyzed by using the extended Freundlich and the Sheindorf-Rebuhn-Sheintuch (SRS) models for multicomponent adsorption systems (39–41).

**Table 4.** Freundlich and D-R isotherm parameters for AB adsorption from binary solutions

| | | Freundlich parameters | | | D-R parameters | | |
|---|---|---|---|---|---|---|---|
| | $T$ (K) | $n_1$ | $k_F$ mmol/g | $r$ | $K_{D\text{-}R} \times 10^3$ mol$^2$/kJ$^2$ | $q_m$ mmol/g | $r$ |
| 0.05 mM TA | 298 | 0.65 | 0.28 | 0.94 | 4.49 | 0.54 | 0.94 |
| | 308 | 0.48 | 0.19 | 0.99 | 3.16 | 0.32 | 0.99 |
| | 318 | 0.42 | 0.14 | 0.81 | 1.38 | 0.08 | 1.00 |
| | 328 | 0.63 | 0.28 | 0.99 | 3.65 | 0.57 | 0.99 |
| 0.10 mM TA | 298 | 0.80 | 0.25 | 0.95 | 6.11 | 0.90 | 0.98 |
| | 308 | 0.97 | 0.57 | 0.95 | 6.93 | 2.64 | 0.98 |
| | 318 | 0.30 | 0.07 | 0.86 | 1.98 | 0.07 | 0.93 |
| | 328 | 0.30 | 0.06 | 0.91 | 1.84 | 0.09 | 0.96 |



## Extended Freundlich Model

The extended Freundlich isotherm for binary adsorption systems can be formulated as follows:

$$q_{e,1} = \frac{k_{F,1} C_{e,1}^{n_1 + x_1}}{C_{e,1}^{x_1} + y_1 C_{e,2}^{z_1}} \tag{18}$$

where, $k_{F,1}$ and $n_1$ are Freundlich isotherm constants of the first component in single solute system and other three parameters ($x_1$, $y_1$, and $z_1$) are its extended Freundlich constants. $q_{e,1}$ is the equilibrium adsorption of the first component; $C_{e,1}$ and $C_{e,2}$ are equilibrium concentrations of the first and the second components in binary solutions, respectively. The equilibrium adsorption of AB in the presence of 0.05 and 0.1 mM TA has been calculated by nonlinear regression from Eq. (18) by minimizing standard deviations between the observed and the calculated $q_{e,1}$ values. The calculated amounts of AB adsorbed ($q_{e,1,cal}$) together with isotherm parameters are presented in Table 5. The parameters, $x_1$, $y_1$, and $z_1$ have been calculated using $k_{F,1}$ and $n_1$ values corresponding to low concentration region whereas $x'_1$, $y'_1$, and $z'_1$ correspond to $k'_{F,1}$ and $n'_1$ for higher concentrations in Table 2. As can be seen from the $\sigma$ values, the extended Freundlich isotherm adequately well fits to equilibrium data of AB in binary solutions.

**Table 5.** Extended Freundlich isotherm parameters and calculated values of AB adsorbed

| | | $q_{1,cal}$ mmol/g | | | |
|---|---|---|---|---|---|
| | $C_0$ mM | 298 K | 308 K | 318 K | 328 K |
| 0.05 mM TA | 0.05 | 0.0033 | 0.0045 | 0.0005 | 0.0025 |
| | 0.10 | 0.0099 | 0.0039 | 0.0001 | 0.0049 |
| | 0.15 | 0.0148 | 0.0119 | 0.0032 | 0.0095 |
| | 0.20 | 0.0200 | 0.0190 | 0.0022 | 0.0163 |
| | 0.30 | 0.0200 | 0.0296 | 0.0278 | 0.0277 |
| $\sigma$ | | 0.006 | 0.059 | 0.322 | 0.108 |
| $x_1$ | | 0.80 | −1.23 | – | −0.13 |
| $y_1$ | | 0.01 | 0.01 | – | 0.01 |
| $z_{1.}$ | | 0.10 | 0.10 | – | 0.10 |
| $x'_1$ | | −0.84 | −0.23 | 1.35 | 0.09 |
| $y'_1$ | | 0.01 | 1.80 | 0.01 | 2.00 |
| $z'_{1.}$ | | 0.10 | 0.10 | 0.10 | 0.20 |
| 0.10 mM TA | 0.05 | 0.0033 | 0.0033 | 0.0003 | 0.0031 |
| | 0.10 | 0.0098 | 0.0033 | 0.0019 | 0.0031 |
| | 0.15 | 0.0118 | 0.0175 | 0.0020 | 0.0042 |
| | 0.20 | 0.0186 | 0.0192 | 0.0043 | 0.0129 |
| | 0.30 | 0.0237 | 0.0246 | 0.0249 | 0.0279 |
| $\sigma$ | | 0.005 | 0.068 | 0.316 | 0.146 |
| $x_1$ | | 1.50 | 2.27 | – | 2.07 |
| $y_1$ | | 0.01 | 0.01 | – | 0.01 |
| $z_{1.}$ | | 0.10 | 0.10 | – | 0.10 |
| $x'_1$ | | −0.34 | −0.63 | 0.79 | −0.12 |
| $y'_1$ | | 18.00 | 24.00 | 0.01 | 6.60 |
| $z'_{1.}$ | | 0.10 | 0.100 | 0.10 | 0.1 |



### Sheindorf-Rebuhn-Sheintuch (SRS) Model

The SRS equation is a multicomponent adsorption isotherm that assumes each component individually obeys the Freundlich isotherm. A general SRS equation for a component $i$ in an $N$ component system can be written as follows:

$$q_{e,i} = k_{F,i} C_{e,i} \left( \sum_{j=1}^{N} a_{ij} C_{e,j} \right)^{n_i - 1} \tag{19}$$

where, $k_{F,i}$ and $n_i$ are Freundlich constants for the single component system, $a_{ij}$ is the competition coefficient which describes the inhibition

to the adsorption of component $i$ by component $j$. Competition coefficient $a_{ij}$ for the binary system is reciprocal of $a_{ij}$ and can be determined from the experimental data.

The SRS parameters for AB adsorption in the presence of TA have been calculated by minimizing $\sigma$ values and presented in Table 6. As can be seen from Table 6, $a'_{1,2}$ calculated from the individual Freundlich parameters ($k'_F$ and $n'$) in Table 2 equals to $1/a'_{2,1}$ for high concentration region. In this region, $a'_{1,2} < 1$ and $a'_{2,1} > 1$ indicate that AB adsorption is inhibited by TA at high concentrations. On the other hand, since AB adsorption increases in the presence of TA it does not obey SRS equation at low concentration region. However, the amount of AB could be calculated from the SRS equation by assuming $a_{1,2}$ and $a_{2,1}$ are independent variables for the enhancement of adsorption. The values of $a_{2,1} < a_{1,2}$ calculated from $k_{F,1}$ and $n_1$ parameters in Table 2 may be considered as an indication for enhancement of adsorption by the second component.



**Table 6.** The SRS isotherm parameters and calculated values of AB adsorbed

| | | $q_{1,cal}$ mmol/g | | | |
|---|---|---|---|---|---|
| | $C_0$mM | 298 K | 308 K | 318 K | 328 K |
| 0.05 Mm TA | 0.05 | 0.0043 | 0.0049 | 0.0049 | 0.0020 |
| | 0.10 | 0.0100 | 0.0086 | 0.0028 | 0.0098 |
| | 0.15 | 0.0146 | 0.0087 | 0.0103 | 0.0147 |
| | 0.20 | 0.0200 | 0.0182 | 0.0090 | 0.0194 |
| | 0.30 | 0.0173 | 0.0285 | 0.0246 | 0.0286 |
| $\sigma$ | | 0.061 | 0.057 | 0.186 | 0.003 |
| $a_{1,2}$ | | 0.28 | 1.00 | 8.00 | $1.00 \times 10^{-2}$ |
| $a_{2,1}$ | | $5.10 \times 10^{-3}$ | 0.10 | 0.30 | $4.0 \times 10^{-3}$ |
| $a'_{1.2}$ | | 0.08 | $8.00 \times 10^{-3}$ | | 0.30 |
| $a'_{2,1}$ | | $1.25 \times 10$ | $1.25 \times 10^2$ | | 3.33 |
| 0.10 mM TA | 0.05 | 0.0049 | 0.0032 | 0.0004 | 0.0049 |
| | 0.10 | 0.0088 | 0.0031 | 0.0064 | 0.0100 |
| | 0.15 | 0.0070 | 0.0114 | 0.0066 | 0.0022 |
| | 0.20 | 0.0158 | 0.0137 | 0.0102 | 0.0092 |
| | 0.30 | 0.0243 | 0.0244 | 0.0281 | 0.0249 |
| $\sigma$ | | 0.040 | 0.069 | 0.169 | 0.203 |
| $a_{1,2}$ | | $1.00 \times 10^{-3}$ | $2.8 \times 10^{-3}$ | | |
| $a_{2,1}$ | | $5.00 \times 10^{-4}$ | $2.00 \times 10^{-4}$ | | |
| $a'_{1,2}$ | | $1.20 \times 10^{-5}$ | $1.30 \times 10^2$ | $1.80 \times 10$ | $5.10 \times 10^{-6}$ |
| $a'_{2,1}$ | | $8.33 \times 10^4$ | $7.69 \times 10^{-3}$ | $5.55 \times 10^{-2}$ | $1.96 \times 10^5$ |

## Relation between AB and TA Adsorption

The amount of TA adsorbed ($q_{e,2}$) in the presence of 0.05 mM and 0.10 mM TA were also determined corresponding to AB loading ($q_{e,1}$) and presented in Figs. 5a′ and 5b′, respectively. Although experimental equilibrium data of AB are quite well described by the extended Freundlich and the SRS equations standard deviations for TA increase up to 0.55 (not shown here). This may be arising from the enhancement of experimental values instead of an inhibition in the model predictions. However, a polynomial relation is observed between experimental equilibrium adsorption values of AB and TA which, can be formulated as follows:

$$q_{e,2} = Aq_{e,1}^3 + Bq_{e,1}^2 + Cq_{e,1} + D \tag{20}$$

where, *A, B, C*, and *D* are polynomial coefficients and their values are presented in Table 7. As clearly shown in both figures and the polynomial coefficients, the shape of curves obtained from 0.05 mM and 0.10 mM TA solutions are opposite directions. In the presence of 0.05 M TA in binary solution, $q_{e,2}$ values increase with respect to the single solution (i.e., $q_{e,1} = 0$) indicating favorable TA-AB interactions at low AB coverage. The reverse effect is observed at higher AB loadings suggesting that orientation of AB adsorbed on the surface at low loadings is in opposite directions with those of high loadings. It can be concluded that from these observations the organophilic character of the adsorbent surface changes depending on the AB loading and polynomial maximum and/or minimum appear at the points of organophilic-organophobic change. The opposite shape of the polynomial curves in Figs. 5a and 5b suggest that solute-solute interactions in the solution phase also contribute to

**Table 7.** Polynomial coefficients for TA adsorption in the presence of AB

| TA | *T* (K) | *A* | *B* | *C* | *D* |
|---|---|---|---|---|---|
| 0.05 mM | 298 | 394.9 | −18.8 | 0.293 | 0.0009 |
| | 308 | 273.4 | −14.3 | 0.270 | 0.0007 |
| | 318 | 89.7 | −3.6 | 0.109 | 0.0007 |
| | 328 | 471.0 | −12.2 | 0.074 | 0.0000 |
| 0.10 mM | 298 | −3054 | 109.4 | −0.749 | 0.0025 |
| | 308 | −2138 | 84.5 | −0.670 | 0.0022 |
| | 318 | −2028 | 73.7 | −0.508 | 0.0020 |
| | 328 | −2514 | 96.8 | −0.798 | 0.0019 |

TA adsorption. The TA molecules in 0.05 and 0.10 mM solutions are adsorbed with their opposite poles on the adsorbent surface loaded with the same amounts of AB.

As is seen in Figs. 5a′ and 5b′, although the parameters presented in Table 2, 3, and 4 show no specific trend for the effect of temperature equilibrium adsorption of TA under experimental conditions regularly increases with temperature in binary solutions. Thus, the curves may be useful for determination of optimum conditions for the separation or the binary adsorption of two dyes.

## Thermodynamic Calculations

Free energy changes ($\Delta G^0$) in the systems were calculated according to Eq. (17) using K constants of D-R equation in Tables (2–4) and presented in Fig. 6a depending on temperature. In general, the values of $\Delta G^0$ show a minimum at around 308 K indicating dye adsorption is more spontaneous at this temperature. These results are consistent with the isotherm curves constructed in Figs. 3a, 4, and 5a, which show maximum dye adsorption at 308 K. On the other hand, as it is seen in Fig. 5b, AB adsorption in the presence of 0.10 mM TA regularly increases with temperature under experimental conditions and this behavior is reflected in its corresponding curve in Fig. 6a.

The shapes of $\Delta G^0$ vs. $T$ curves may be arisen from the changes in exothermic and endothermic nature of adsorption as a result of entropy changes arising from orientation of the dye molecules on adsorbent surface.

The standard entropy was evaluated from $\Delta G^0 - T$ curves using the following well-known equation:

$$-\Delta S^0 = \left(\frac{\partial \Delta G^0}{\partial T}\right)_P \tag{21}$$

By substituting these $\Delta S^0$ values in the following equation, the standard enthalpy $\Delta H^0$ were calculated.

$$\Delta H^0 = \Delta G^0 + T\Delta S^0 \tag{21}$$

The plots of $\Delta S^0$ and $\Delta H^0$ vs. $T$ were represented in Figs. 6b and 6c, respectively. $\Delta S^0$ and $\Delta H^0$ show a linear dependency on temperature with a negative slope with one exception as mentioned above. The adsorption process for TA in single solution and for AB in the presence of high TA concentration is of an endothermic nature while it converts

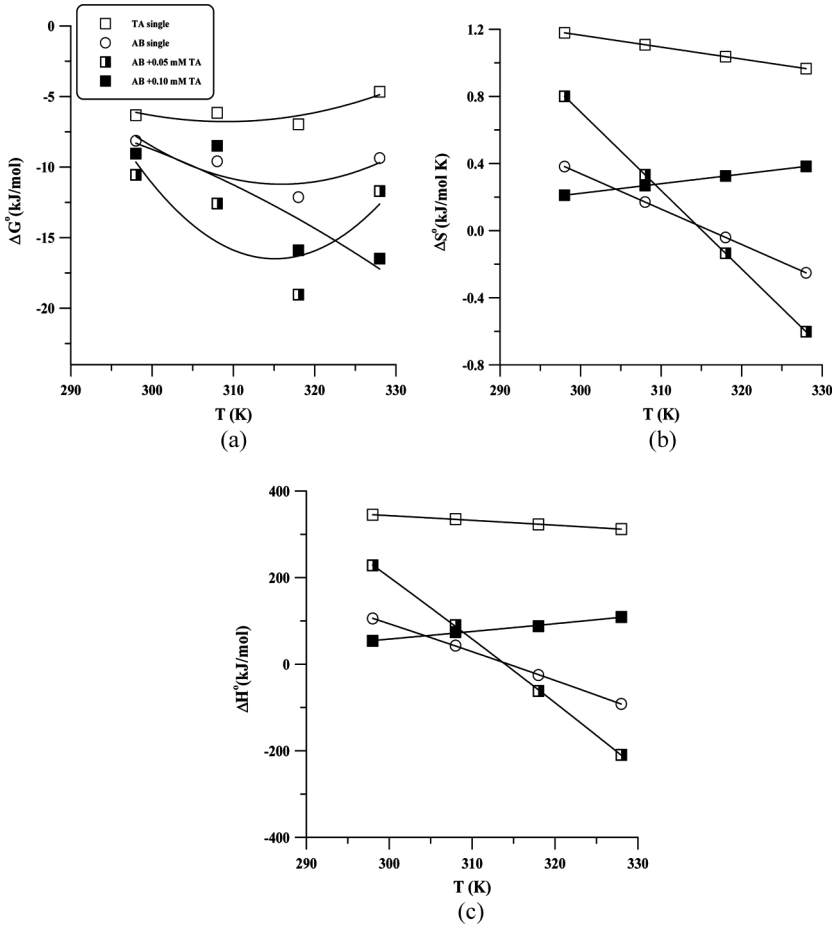


*Figure 6.* Temperature dependency of thermodynamic parameters (a) Free energy (b) entropy and (c) enthalpy changes for single and binary dye adsorption systems.

into exothermic in single AB and in the presence of TA at low concentration. This suggests that AB adsorption is more favorable than TA. An increase in AB concentration varies the sign of enthalpy from positive to negative. Similar trend is also observed for the sign of entropy values as the temperature increases. As a result of more regular orientation, rotational and vibrational motions of adsorbed dye molecules, which are responsible for enthalpy changes, are restricted (42). The reverse effect of temperature on entropy changes is in agreement with experimental observations in the presence of 0.10 mM TA in binary solute system.

## CONCLUSIONS

Optimum conditions for adsorptive removal of AB and TA on FA have been evaluated from kinetic and equilibrium experiments performed in single and binary dye solutions.

- Equilibrium amounts of dyes adsorbed calculated from pseudo-second-order kinetic model for binary solutions are higher than those found for their corresponding single solutions because of solute – solute interactions between two dyes.
- Similar relation is also observed on initial parts of the AB isotherm curves constructed in the presence of TA whereas AB adsorption decreases in concentrated binary solutions.
- Polynomial relation observed between amounts of adsorbed of two dyes reflects suitable conditions for single or binary adsorption from mixed solutions. Especially, the minima on the curves at the highest temperature correspond to separation of AB on the FA.
- Isotherm curves are quite well defined with the Freundlich and the D-R isotherm equations. Equilibrium adsorption of AB in binary solutions could also be calculated from the extended Freundlich and the Sheindorf-Rebuhn-Sheintuch (SRS) models by using the individual Freundlich constants in single solutions.
- The amount of AB adsorbed on FA under experimental conditions is much higher than those found for other acid dyes in the literature while TA adsorption falls in the same range.



Consequently, both AB and TA are successfully removed by fly ash from colored solutions. The kinetic and equilibrium parameters might be useful for designing a treatment plant for color removal from both single and binary solutions.

Based on the data obtained in this study, further experiments are planned for adsorption of other acid dyes from binary solutions using fly ash as an adsorbent.

## NOMENCLATURE

| | |
|---|---|
| $a$ | parameter of the pseudo-second-order model |
| AB | acid blue 113 |
| $a_{ij}$ | competition coefficients of component $i$ by component $j$, dimensionless |
| $a'_{ij}$ | competition coefficients of component $i$ by component $j$ for the second part of isotherm, dimensionless |

| | |
|---|---|
| $b$ | parameter of the pseudo-second-order model |
| $B$ | time coordinate, 1/s |
| $h_s$ | initial sorption rate, mmol/g s |
| $C_0$ | initial concentration of adsorbate in solution, mmol/l |
| $C_e$ | equilibrium concentration in single component system, mmol/l |
| $C_{e,i}$ | equilibrium concentration of each component in binary solution, mmol/l |
| $C_t$ | adsorbate concentration in solution at time t, mmol/l |
| $D_i$ | effective diffusion coefficient, $m^2/s$ |
| $E$ | mean adsorption energy, kJ/mol |
| FA | fly ash |
| $F_t$ | fractional attainment at equilibrium |
| $G^0$ | Standard free energy |
| $H^0$ | Standard enthalpy |
| $k_2$ | pseudo-second-order rate constant, g/mmol s |
| $K_{D\text{-}R}$ | The D-R isotherm constant related to the mean adsorption energy, $mol^2/kJ^2$ |
| $k_F$ | pre-exponential Freundlich isotherm constant of the single component system, mmol/g |
| $k'_F$ | pre-exponential Freundlich isotherm constant of the single component system for the second part of isotherm, mmol/g |
| $k_{F,i}$ | pre-exponential Freundlich constant of individual isotherm of each component, mmol/g |
| $m$ | mass of adsorbent, g |
| $n$ | Freundlich exponent of the single component, dimensionless |
| $n'$ | Freundlich exponent of the single component for the second part of isotherm, dimensionless |
| $n_e$ | number of experimental observations |
| $n_i$ | individual Freundlich exponent of each component, dimensionless |
| $q_e$ | amount of dye adsorbed at equilibrium, mmol/g |
| $q_{e,i}$ | equilibrium solid phase concentration of each component in binary solution, mmol/g. |
| $q_{e,cal}$ | calculated value of solid phase concentration of adsorbate at equilibrium, mmol/g. |
| $q_{e,\exp}$ | experimental value of solid phase concentration of adsorbate at equilibrium, mmol/g. |
| $q_m$ | adsorption capacity predicted from isotherm parameters, mmol/g |
| $q_t$ | solid phase concentration of adsorbate at time $t$, mmol/g. |
| $q_{t,\exp}$ | experimental value of solid phase concentration of adsorbate at time t, mmol/g. |

$q_{t,cal}$ calculated value of solid phase concentration of adsorbate at time t, mmol/g.
$R$ universal gas constant, kJ/mol K
$r$ correlation coefficient
$S^0$ Standard enthalpy
$t$ time, min
$T$ absolute temperature, K
TA tartrazine
$V$ solution volume, l
$x_i$ extended Freundlich isotherm parameter for component $i$
$y_i$ extended Freundlich isotherm parameter for component $i$
$z_i$ extended Freundlich isotherm parameter constant for component $i$

**Greek Symbols**

$\alpha$ parameter of the pseudo-second-order model
$\beta$ parameter of the pseudo-second-order model
$\epsilon$ Polanyi potential, kJ/mol
$\sigma$ standard deviation



## REFERENCES

1. Haberhauer, G.; Pfeiffer, L.; Gerzabek, M.H. (2000) Influence of molecular structure on sorption of phenoxyalkanoic herbicides on soil and its particle size fractions. *J. Agr. Food Chem.*, *48*: 3722.
2. Janos, P.; Buchtova, H.; Ryznarov, M. (2003) Sorption of dyes from aqueous solutions onto fly ash. *Water Res.*, *37*: 4938.
3. Rao, V.V.B.; Rao, S.R.M. (2006) Adsorption studies on treatment of textile dyeing industrial effluent by flyash. *Chem. Eng. J.*, *11*: 677.
4. Woolard, C.D.; Strong, J.; Erasmus, C.R. (2002) Evaluation of the use of modified coal ash as a potential sorbent for organic waste streams. *Appl. Geochem.*, *17*: 1159.
5. Wang, S.; Boyjoo, Y.; Choueib, A. (2005) A comparative study of dye removal using fly ash treated by different methods. *Chemosphere*, *60*: 1401.
6. Wang, S.; Boyjoo, Y.; Choueib, A.; Zhu, Z.H. (2005) Removal of dyes from aqueous solution using fly ash and red mud. *Water Res.*, *39*: 129.
7. Wang, S.; Soudi, M.; Li, L.; Zhub, Z.H. (2006) Coal ash conversion into effective adsorbents for removal of heavy metals and dyes from wastewater. *J. Hazard. Mater. B.*, *133*: 243.
8. Kumar, K.V.; Ramamurthi, V.; Sivanesan, S. (2005) Modeling the mechanism involved during the sorption of methylene blue onto fly ash. *J. Colloid Interface. Sci.*, *284*: 14.
9. Li, L.; Wang, S.; Zhu, Z. (2006) Geopolymeric adsorbents from fly ash for dye removal from aqueous solution. *J. Colloid Interface Sci.*, *300*: 52.

10. Talman, R.Y.; Atun, G. (2006) Effects of cationic and anionic surfactants on the adsorption of toluidine blue onto fly ash. *Colloid Surf. A.*, *281*: 15.
11. Matheswaran, M.; Karunanithi, T. (2007) Adsorption of Chrysoidine R by using fly ash in batch process. *J. Hazard. Mater.*, *145* (25): 154.
12. Wang, S.; Li, H. (2005) Dye adsorption on unburned carbon: Kinetics and equilibrium. *J. Hazard. Mater.*, *126*: 71.
13. Ravikumar, K.; Krishnan, S.; Ramalingam, S.; Balu, K. (2007) Optimization of process variables by the application of response surface methodology for dye removal using a novel adsorbent. *Dyes Pigm.*, *72*: 66.
14. Eren, Z.; Acar, F.N. (2006) Adsorption of Reactive Black 5 from aqueous solution: Equilibrium and kinetic studies. *Desalination*, *194*: 1.
15. Mittal, A.; Mittal, J.; Kurup, L. (2006) Adsorption isotherms, kinetics and column operations for the removal of hazardous dye, Tartrazine from aqueous solutions using waste materials-bottom ash and de-oiled soya, as adsorbents. *J. Hazard. Mater. B.*, *136*: 567.
16. Mane, V.S.; Mall, I.D.; Srivastava, V.C. (2007) Kinetic and equilibrium isotherm studies for the adsorptive removal of Brilliant Green dye from aqueous solution by rice husk ash. *J. Environ. Manage.*, *84* (4): 390.
17. Mall, I.D.; Srivastava, V.C.; Agarwal, N.K.; Mishra, I.M. (2005) Removal of congo red from aqueous solution by bagasse fly ash and activated carbon: Kinetic study and equilibrium isotherm analyses. *Chemosphere.*, *61*: 492.
18. Mall, I.D.; Srivastava, V.C.; Agarwal, N.K. (2006) Removal of Orange-G and Methyl Violet dyes by adsorption onto bagasse fly ash kinetic study and equilibrium isotherm analyses. *Dyes Pigm.*, *69*: 210.
19. Mane, V.S.; Mall, I.D.; Srivastava, V.C. (2007) Use of bagasse fly ash as an adsorbent for the removal of brilliant green dye from aqueous solution. *Dyes Pigm.*, *73*: 269.
20. Erol, M.; Genç, A.; Öveçoğlu, M.; Yücelen, E.; Küçükbayrak, S.; Taptik, Y. (2000) Characterization of a glass-ceramic produced from thermal power plant fly ashes. *J. Eur. Ceram. Soc.*, *20*: 2209.
21. Shu, H.Y.; Chang, M.C.; Fan, H.J. (2005) Effects of gap size and UV dosage on decolorization of C.I. Acid Blue 113 wastewater in the UV/$H_2O_2$ process. *J Hazard. Mater. B.*, *118*: 205.
22. Jain, A.K.; Gupta, V.K.; Bhatnagar, A.; Suhas. (2003) Utilization of industrial waste products as adsorbents for the removal of dyes. *J. Hazard. Mater. B.*, *10*: 131.
23. Al-Sarawya, A.; Rasheda, I.G.; Hannab, M.A.; Walia, M.F.K. (2005) Removal of some 4-pyrazolone dyes from aqueous solutions by adsorption onto different types of carbon. *Desalination*, *186*: 129.
24. Mittal, A.; Mittal, J.; Kurup, L. (2006) Adsorption isotherms, kinetics and column operations for the removal of hazardous dye, Tartrazine from aqueous solutions using waste materials-bottom ash and de-oiled soya, as adsorbents. *J. Hazard. Mater. B.*, *136*: 567.
25. Patel, R.; Suresh, S. (2006) Decolourization of azo dyes using magnesium–palladium system. *J. Hazard. Mater. B.*, *137*: 1729.

26. Mittal, A.; Kurup, L.; Mittal, J. (2007) Freundlich and Langmuir adsorption isotherms and kinetics for the removal of Tartrazine from aqueous solutions using hen feathers. *J. Hazard. Mater. B.*, *146* (1–2): 243.
27. Huddleston, J.G.; Willauer, H.D.; Boaz, K.R.; Rogers R.D. (1998) Separation and recovery of food coloring dyes using aqueous biphasic extraction chromatographic resins. *J. Chromatogr. B.*, *711*: 237.
28. Tugcu, N.; Cramer, S.M. (2005) The effect of multi-component adsorption on selectivity in ion exchange displacement systems. *J. Chromatogr. A.*, *1063*: 15.
29. Ho, Y.S. (2005) Effect of pH on lead removal from water using tree fern as the sorbent. *Bioresour. Technol.*, *96*: 1292.
30. Ho, Y.S.; McKay, G. (1999) Pseudo-second order model for sorption processes. *Process Biochem.*, *34*: 451.
31. Boyd, G.E.; Adamson, A.W.; Myers, L.S. (1947) The exchange adsorption of ions from aqueous solutions by organic zeolites. II.Kinetics. *J. Am. Chem. Soc.*, *69*: 2836.
32. Reichenberg, D. (1953) Properties of ion-exchange resins in relation to their structure.III. kinetics of exchange. *J. Am. Chem. Soc.*, *75*: 589.
33. Srivastava, V.C.; Mall, I.D.; Mishra, I.M. (2008) Adsorption of toxic metal ions onto activated carbon. Study of sorption behaviour through characterization and kinetics. *Chem. Eng. Process.* (In Press, doi:10.1016/j.cep.2007.04.006.)
34. Somasundaran, P.; Fuerstenau, D.W. (1966) Mechanisms of alkyl sulfonate adsorption at the alumina– water interface. *J. Phys. Chem.*, *70*: 90.
35. Huang, L.; Somasundaran, P. (1996) The change in structure of surfactant aggregates during adsorption/desorption processes and its effect on the stability of alumina suspension. *Colloid Surf. A.*, *117* (3): 235.
36. Healya, T.W.; Somasundaranb, P.; Fuerstenau D.W. (2003) The adsorption of alkyl and alkylbenzene sulfonates at mineral oxide–water interfaces. *Int. J. Miner. Process.*, *72*: 3.
37. Atkin, R.; Craig, V.S.J.; Wanless, E.J.; Biggs, S. (2003) Mechanism of cationic surfactant adsorption at the solid–aqueous interface. *Adv. Colloid Interface Sci.*, *103*: 219.
38. Pura, S.; Atun, G. (2005) Enhancement of nitrophenol adsorption in the presence of anionic surfactant and the effect of the substituent position. *Colloid Surf. A.*, *253*: 137.
39. Srivastava, V.C.; Mall, I.D.; Mishra, I.M. (2006) Modelling individual and competitive adsorption of cadmium (II) and zinc(II) metal ions from aqueous solution onto bagasse fly ash. *Sep. Sci. Technol.*, *41*: 2685.
40. Srivastava, V.C.; Mall, I.D.; Mishra, I.M. (2008) Antagonistic competitive equilibrium modeling for the adsorption of ternary metal ions mixtures onto bagasse fly ash. *Ind. Eng. Chem. Res.*, *47* (9): 3129.
41. Srivastava, V.C.; Mall, I.D.; Mishra, I.M. (2006) Equilibrium modelling of single and binary adsorption of cadmium and nickel onto bagasse fly ash. *Chem. Eng. J.*, *117* (1): 79.
42. Hisarli, G. (2005) The effects of acid and alkali modification on the adsorption performance of fuller's earth for basic dye. *J. Colloid Interface. Sci.*, *281*: 18.